Supplemental Data

Gating Mechanism of the Influenza A M2 Channel

Revealed by 1 and 2D IR Spectroscopies

Joshua Manor, Prabuddha Mukherjee, Yu-Shan Lin, Hadas Leonov, James L. Skinner, Martin T. Zanni, and Isaiah T. Arkin

SUPPLEMENTAL EXPERIMENTAL PROCEDURES

Sample Preparation

Peptide synthesis
The peptides used in this work encompass the transmembrane domain of M2 and correspond to residues Ser22 to Leu46: SSDPLVVAASIIGILHLILWILDRL [1]. The peptides were synthesized using standard solid-phase N-(9-fluorenyl methoxycarbonyl) chemistry, cleaved from the resin with trifluoroacetic acid, and lyophilized. Each peptide was labelled using 1-$^{13}C=^{18}O$ amino acids, using ^{13}C labelled amino acids precursors (Cambridge Isotopes Laboratories, Andover, MA) at positions indicated in Fig. 1a using procedures descried elsewhere in detail [2, 3].

Peptide purification
0.5 mg of the crude synthesis was dissolved in 0.75 ml of trifluoroacetic acid, and injected into a 20 ml Jupiter 5 C4-300 Å column (Phenomex, Cheshire, UK) equilibrated with 80% H2O, 8% (w/v) acetonitrile and 12% (v/v) 2-propanol. Peptide elution was achieved with a linear gradient to a final solvent composition of 40% acetonitrile and 60% 2-propanol. All solvents contained 0.1% (v/v) trifluoroacetic acid.

Peptide reconstitution
1 mg of peptide was co-solubilizied with 10 mg of 1,2-dimyristoyl-sn-glycero-3-phosphocholine lipids (Avanti polar lipids, Alabaster Al) in 1 ml of 1,1,1,3,3,3-hexafluoro-2-propanol (Merck, Whitehouse Station, NJ) for 2 hours at 37°. The solution was desiccated overnight and liposomes were prepared by hydration of the sample in 2 ml water. Reconstituted liposomes were sonicated in a probe-type sonicator for 2 minutes at 100 Watt (pulses given every 2 seconds). Liposomes were extruded through 0.2 μm nitrocellulose filter at 37°. Finally the above preparation of M2 has been used by our group in numerous studies [3-7] and has been shown to result in protein that is fully capable of binding amantadine [8].

pH control
In the ATR-FTIR work, HCl, NaOH and phosphate buffer saline (PBS) were used to bring the solution to a final pH of 4, 7 or 9, respectively. The pH was monitored throughout the entire process, including during the removal of the bulk solvent from the sample before measuring the FTIR spectra, and was found to change only marginally in all three preparations. The three different conditions had no visible effect on the FTIR spectra. HCl-treated preparation is addressed as low pH samples throughout this work, while PBS or NaOH treated preparations are addressed as neutral/basic pH samples. No differences between the results were obtained between preparations with PBS or NaOH. In the 2D IR work, the vesicles resided in excess water. For the closed state measurements, the pH was checked by blotting a small amount on pH paper. For the open state, the sample was buffered to pH 5.

1D FTIR Spectroscopy

ATR-FTIR spectra collection

FTIR spectra were collected on a Nicolet Magna 560 spectrometer (Madison, WI), equipped with a high-sensitivity liquid nitrogen-cooled MCT/A detector. Attenuated total internal reflection (ATR) spectra were measured with a 25-reflection ATR accessory from Graseby Specac (Kent, England) and a wire grid polarizer (0.25 mM; Graseby Specac). 600 μl of sample (ca. 0.5 mg/ml protein and 5 mg/ml lipid) were deposited for 3 hours onto a trapezoidal Ge internal reflection element (50 × 2 × 20 mm) under a stream of dry, CO_2-depleted air. After the instrument was purged with CO_2 and water-depleted air overnight, 1000 interferograms were collected and averaged for every sample. Spectra were processed with 1-point zero filling and Happ-Genzel apodization. Peaks in the region between 1520 cm^{-1} and 1800 cm^{-1} were approximated by corresponding Lorentzian and Voigt functions and integrated separately. Amide I related peaks were chosen as Lorentz approximation and lipid related peaks as Voigt.

Lipid bilayer mosaicity estimation by X-ray Scattering

The same samples used for the ATR-FTIR spectroscopy, were also used to obtain the orientational distribution of the bilayer stacks as described elsewhere in detail [9]. Briefly, a scattering profile of the peptide reconstituted in lipid bilayers was obtained in order to determine the location of the first Bragg peak. Subsequently, the angle of the X-ray source and detector are set according to the first Bragg reflection (Bruker AXS equipped with Cu X-ray tube, preformed at the nano-characterization institute, Hebrew university, Jerusalem, Israel). The sample is then gradually tilted (χ-scanned) around an axis perpendicular to the X-ray beam. The intensity profiles are then compared (each profile with a different χ angle) in the following manner: A function of the maximal intensity of each of the fitting function (for each χ scan) is obtained and approximated by a Gaussian curve. The width of a Gaussian approximation constitutes the orientational distribution (mosaicity) of the bilayer.

θ angle experimental derivation

Dichroic ratios were calculated by dividing absorption obtained using parallel-polarized light (0°) by that obtained when using perpendicular-polarized light (90°). When the absorption, using 90°-polarized light was not sufficiently strong, 45°-polarized light was used. The angle between the transition dipole moment of the amide I mode and the membrane normal (the angle θ) was calculated from the dichroic ratio R, using the following equation [9]:

$$R = \frac{E_z K_z + E_x K_x}{E_y K_y} \qquad (1)$$

whereby E_x, E_y and E_z are the axial electric field components given by Harrick [10]. K_x, K_y and K_z are the integrated absorption coefficients, which are the axial components of the transition dipole moment, squared, and are given by

$$K_x = K_y = \frac{1}{4}(1 - e^{-2\sigma^2} Cos[\theta]) \qquad (2)$$

and

$$K_z = \frac{1}{2}(1 + e^{-2\sigma^2} Cos[\theta]) \qquad (3)$$

whereby σ, is the sample mosaicity determined in the X-ray scattering experiments. Finally combing equations 1 through 3, incorporating the exact expressions for the electric field components [10], yields the final equation relating the dichroism, R to the angle between the transition dipole moment and the bilayer normal θ, as follows:

$$R = \frac{Cos[2\theta]\,(n^2 + Sin^2[\xi]\,) - e^{2\sigma^2}\,(n^2 - 3\,Sin^2[\xi])}{(e^{2\sigma^2} - Cos[2\theta])\,(-n^2 + (1+n^2)\,Sin^2[\xi]^2)} \qquad (4)$$

whereby n is the ratio between the refractive indices of the sample and the Ge internal reflection element (1.43 and 4, respectively) and ξ is the angle of incidence between the electric field component and the internal reflection element (45°).

θ angle calculation

To calculate θ from a given structure (used also in the rigid body refinement procedure described below), the transition dipole moment (TDM) of the amide I vibrational mode position was calculated explicitly using the geometry (see Fig. 1d)

described by Torii and co-workers [11]. In brief, a vector was constructed for each amino acid of interest to represent the TDM: starting at 0.868 Å distant to the carbon atom in the carbonyl bond direction, and ending at a distance of 0.505 Å from the carbon atom in the C-N direction (lying completely in the peptidic plane). The projection of this vector with the *z* axis (a vector representing the normal to the membrane plane) is the angle Θ.

Molecular Refinement

Model construction
The channel models presented in this work were constructed by a rigid-body refinement method, using the data measured by the FTIR as follows: An ideal helix was aligned such that its director coincided with the membrane's normal. The helix was then rotated and tilted until maximal agreement with the experimental data was achieved, for each set of data (acidic or neutral pH). Specifically, the helix was tilted in one degree increments, from 0° to 90° and for each tilt angle, the helix was rotated by 360° in one degree increments. For each of the 32,400 tilt and rotation angle states, the local Θ angle was calculated for the ten labelled amino acids of the helix. The sum of the errors for all ten measured θ angles relative to the FTIR-measured angles was then calculated. Thus, each state holds a penalty that corresponds to the distance of the state from the FTIR data. The state with the minimal penalty was selected to represent the 3D interpretation of the FTIR-measured data for each pH. Similarly. Supplemental Figure 6 shows the same refinement taking into account the penalty of individual amino acids.

Construction of the transmembrane M2 tetramer
The outcome of the rigid-body refinement was duplicated three times to generate the four chains of the tetramer. Each helix was centred along with its X-ray derived matching chain (structure 3KBD [12], bundle axis aligned to membrane normal). The helices were then turned around the membrane normal to yield the structure with the minimal RMSD from the corresponding x-ray chain. Note that neither the tilt nor the rotation angle was changed, and as such the experimental constraints from the FTIR spectroscopy were maintained. Finally the constructed tetramer was energy-minimized using GROMACS, g96 vacuum force-field [13].

2D IR Spectroscopy

Data Collection and Fits
The experimental procedure for collecting heterodyned 2D IR spectra is given in detail elsewhere [14]. In brief, three femtosecond Fourier transform limited pulses (1.2 J, 150 cm^{-1} bandwidth, 400 nJ) with wavevectors k_1, k_2, and k_3 were incident on the sample and the signal was monitored in the $-k_1 + k_2 + k_3$ phase matching direction with a fourth local oscillator pulse (~2 nJ) that measured the time-dependence of the emitted signal in a balanced heterodyne detection system. This choice of time-delays and phase matching results in the measurement of a photon echo signal. All four pulses have identical polarizations. The time delay between pulses in the directions k_1 and k_2 is t_1, between k_2 and k_3 is t_2, and between k_3 and the local oscillator pulse is t_3. The 2D IR data set was generated by collecting the heterodyned signal as a function of t_3 and t_1 which were both scanned 2500 fs in 18 fs steps for a fixed t_2. The 2D IR spectra are generated by Fourier transforming the time-domain data along t_1 and t_3 and the absolute value of the Fourier transformed spectra are reported. To measure the population relaxation times, a series of 2D IR spectra were collected as a function of t_2 while t_3 and t_1 which were scanned over 1500 fs. The intensity of the isotope labelled peak was plotted and fit to a single exponential. The resulting lifetimes are reported in Table S1.

To extract the 2D lineshape of the labelled amide I mode, we follow our previously established fitting procedure of using the Fourier transform of the 3rd-order response in the limit of Bloch dynamics with a pure dephasing time of T_2^* and an inhomogeneous distribution of Δ_0 [15]. The lineshape function in the Bloch limit is given by

$$g(t) = e^{\frac{t}{T_2^*} + \frac{\Delta_0^2 t^2}{2}}. \qquad (5)$$

The rephasing response function is then calculated as[16-18]:

$$R_{123}(t_3,t_1) \sim e^{-2g(t_1)-2g(t_3)+g(t_1+t_3)}\left[e^{-i\langle\omega_{10}\rangle(t_3-t_1)} e^{-\frac{t_1+t_3}{2T_{10}}} - e^{-i(\langle\omega_{21}\rangle t_3 - \langle\omega_{10}\rangle t_1)} e^{-\frac{t_1+t_3}{2T_{10}}} e^{-\frac{t_3}{2T_{21}}} \right] \qquad (6)$$

and the fitting expression in the limit of δ-function pulses is

$$S(\omega_3,\omega_1) = \left| \int_0^\infty dt_1 \int_0^\infty dt_3 e^{i\omega_3 t_3 - i\omega_1 t_1} \,\mathrm{Re}\left[R_{123}(t_3,t_1)\right] \right|. \qquad (7)$$

Here $\langle\omega_{10}\rangle$ is the average transition frequency between states υ=1 and 0 and $\langle\omega_{21}\rangle$ between states υ=2 and 1; T_{10} and T_{21} are the population relaxation times from state υ=1 to 0 and 2 to 1, respectively. Since the population times are similar and long enough that they contribute only a few wavenumbers to the linewidth, we set T_{10} = 600 fs and T_{21} = 400 fs for all the fits (which is consistent with the anti-diagonal widths all being nearly equal.) We used an anharmonicity of Δ = 14 cm^{-1}, the accuracy of which was checked by looking at the negative and positive going peaks in the real parts of the 2D IR spectra (corresponding to the υ=0 to 1 and υ=1 to 2 transitions), which match to <2 cm^{-1} for all of the residues. Explicit pulse widths are used in the actual fitting procedure but have negligible effects on the data. Because the 1-^{13}C=^{18}O modes partially overlaps with the other two amide modes, for the purpose of lineshape fitting, three bands were included in the simulations with independently varied parameters following Eq. 5. The three bands represent the amide I band of the labelled residue, the amide II band, and the amide I ^{13}C natural abundance.

This fitting procedure was followed for all ten labelled peptides at both pH conditions. For each of the ten sites, the sample preparation, collection and fitting procedure was completed three times at each pH for a total of 60 spectra. A representative experimental and simulated 2D IR spectrum for each residue is given in the Supplemental Figures 3 and 5. The results are tabulated in Table I with error bars that are set according to the deviations in the three samples as well as estimates of the systematic errors associated with the fits.

Molecular Simulations

Initial Structure & preparation of the system from MD

The initial structure used in this study was derived from the X-ray homo-tetramer structure, PDB entry 3BKD [12]. The principal axis of the pore was aligned to the membrane normal, and the protein was embedded in a pre-equilibrated 1,2-dimyristoyl-sn-glycero-3-phosphocholine bilayer downloaded from Peter Tieleman's site (moose.bio.ucalgary.ca). The bilayers initially had 128 lipids embedded in 3687 molecules of SPC water [19]. Colliding lipids were automatically removed in range of 1 Å of the protein. After the automatic removal of lipids, a visual inspection was performed, and lipids that interfered with the helical bundle were manually removed.

The structure preparation included two more stages. (i) The original PDB (3BKD) contained crystal water molecules that were represented by oxygen atoms only. Hydrogen atoms were added to each, by placing full a SPC water molecule [19] instead of each such oxygen. (ii) The original PDB contained a residue of Seleno-Methionine (MSE) in each monomer which was changed to a standard Methionine.

According to Cross and co-workers [20], the channel is opened when three Histidines are charged. So, in order to simulate an open channel, three of the four Histidines were protonated. Finally, In order to neutralize the system charge before PME calculations, one Na^+ counter ion randomly replaced a water molecule in the system.

Simulation Steps

Energy Minimization The system underwent energy-minimization in which the crystal waters were positionally restrained in order to retain their original location.

Positional Restraints Following the energy minimization, a gradual positional restraints procedure was applied. The positional restraints began by restraining both lipid and protein atoms by a force of 1000 kJ mol^{-1} nm^{-2} for 20 ps. Then, subsequent simulations were performed, in which this force was gradually decreased to 0. The length of the simulation was linearly dependent on the force, so that it reached a 1ength of 100 ps at F = 0 kJ mol^{-1} nm^{-2}. Furthermore, the steps were decreased by a smaller step size when the force became less stringent. The positional restraints step size was 2 fs, and thus all bonds containing hydrogens were constrained in the system. This process was meant to improve the packing of the lipids around the protein and to gradually equilibrate the protein.

MD simulations

The system was subjected to a 20 ns MD simulation for 3 trials (total of 60 ns) in order to test the convergence of the simulation. The simulations were conducted using version 3.3.1 of the GROMACS MD simulation package [21] employing an extended version of the GROMOS87 force field [22]. 1,2-dimyristoyl-sn-glycero-3-phosphocholine force field parameters were taken from [23]. All simulations were conducted using the LINCS algorithm [24] to constrain bond lengths and angles of hydrogen atoms, allowing a time step of 2 fs. Atomic coordinates were saved every 10 ps. Simulations were conducted at a constant temperature of 310 K. Solvent, lipid, and protein were coupled separately to a Nose-Hoover temperature bath (25,26), with a coupling constant of 0.3 ps. The pressure was kept constant by semisotropic coupling of the system to a Parrinello-Rahman pressure bath [25, 26] of 1 bar, with a coupling constant of 1ps. A cutoff of 1.2 nm was used for van der Waals interactions. Electrostatic interactions were computed by using the PME algorithm [27], with a 1.2 nm cutoff for the direct space calculation. The partial charges for the protein, water, and ions atoms were taken from the GROMOS87 force field [22]. The partial charges of the two different protonation states of the histidine residues involve explicit charge delocalization. Finally, a representative structure was taken from clustering the resulting simulation structures and subjected to a further 1 ns production run with extensive trajectory output for linewidth computations.

Calculated 2D IR lineshapes

To calculate the 2D IR lineshape for each isolated amide I chromophore from MD simulations (see below) the electric field components in the C=O direction on the C and N atoms of each peptide bond, E_C and E_N, were computed with a cut-off radius of 20 Å every 2 fs. The contributions from atoms within three bonds were excluded, following the 1-4 exclusion principle adopted in the MD simulations. An empirical equation is then used to calculate the frequencies from the electric field components [28]:

$$\omega_{10} = 1717 + 4213E_C + 2108E_N \qquad (8)$$

(ω_{10} is in cm^{-1}; E_C and E_N are in atomic units). This frequency map has been applied to an isotope-labelled transmembrane peptide bundle CD3ζ and the calculated 2D IR diagonal widths are in good agreement with experiment [28]. Besides this fully electrostatic method, we applied a second method to calculate the frequencies with the nearest-neighbour contributions computed from a φ-ψ map [29] and the remaining contributions treated using Eqn. (8). The second approach yielded similar 2D IR lineshapes as the first method, and thus its results are not reported in the paper. From the frequency trajectory obtained from a 1-ns long simulation, we calculated the frequency time-correlation function

$$C_{10}(t) = \left\langle \delta\omega_{10}(t)\delta\omega_{10}(0) \right\rangle, \qquad (9)$$

where $\delta\omega_{10}(t)$ is the fluctuation of the instantaneous frequency from its average. The lineshape function $g(t)$ is calculated by its definition

$$g(t) = \int_0^t dt'(t-t')C_{10}(t'). \qquad (10)$$

2D IR magnitude spectra are computed following Eqns. 6 and 7. For each residue, the lineshape is averaged over the four helices and the diagonal width (FWHM) is calculated from a diagonal slice through the maximum (the same procedure as used for analysing the experimental data). To estimate the error, for each residue the

diagonal width is also calculated for each of the four helices and the standard deviation of the mean is calculated.

SUPPLEMENTAL REFERENCES

1. Duff, K.C., and Ashley, R.H. (1992). The transmembrane domain of influenza A M2 protein forms amantadine-sensitive proton channels in planar lipid bilayers. Virology *190*, 485-489.
2. Torres, J., Adams, P.D., and Arkin, I.T. (2000). Use of a new label, (13)==(18)O, in the determination of a structural model of phospholamban in a lipid bilayer. Spatial restraints resolve the ambiguity arising from interpretations of mutagenesis data. J Mol Biol *300*, 677-685.
3. Torres, J., Kukol, A., Goodman, J.M., and Arkin, I.T. (2001). Site-specific examination of secondary structure and orientation determination in membrane proteins: the peptidic (13)C=(18)O group as a novel infrared probe. Biopolymers *59*, 396-401.
4. Kukol, A., Adams, P.D., Rice, L.M., Brunger, A.T., and Arkin, T.I. (1999). Experimentally based orientational refinement of membrane protein models: A structure for the Influenza A M2 H+ channel. J Mol Biol *286*, 951-962.
5. Torres, J., Kukol, A., and Arkin, I.T. (2000). Use of a single glycine residue to determine the tilt and orientation of a transmembrane helix. A new structural label for infrared spectroscopy. Biophys J *79*, 3139-3143.
6. Torres, J., and Arkin, I.T. (2002). C-deuterated alanine: a new label to study membrane protein structure using site-specific infrared dichroism. Biophys J *82*, 1068-1075.
7. Hansen, R.K., Broadhurst, R.W., Skelton, P.C., and Arkin, I.T. (2002). Hydrogen/deuterium exchange of hydrophobic peptides in model membranes by electrospray ionization mass spectrometry. J Am Soc Mass Spectrom *13*, 1376-1387.
8. Astrahan, P., Kass, I., Cooper, M.A., and Arkin, I.T. (2004). A novel method of resistance for influenza against a channel-blocking antiviral drug. Proteins *55*, 251-257.
9. Manor, J., Khattari, Z., Salditt, T., and Arkin, I.T. (2005). Disorder influence on linear dichroism analyses of smectic phases. Biophys J *89*, 563-571.
10. Harrick, N.J. (1965). Electric Field Strengths at Totally Reflecting Interfaces. Journal of the Optical Society of America *55*, 851-&.
11. Torii, H., and Tasumi, M. (1992). Model-Calculations on the Amide-I Infrared Bands of Globular-Proteins. Journal of Chemical Physics *96*, 3379-3387.
12. Stouffer, A.L., Acharya, R., Salom, D., Levine, A.S., Di Costanzo, L., Soto, C.S., Tereshko, V., Nanda, V., Stayrook, S., and DeGrado, W.F. (2008). Structural basis for the function and inhibition of an influenza virus proton channel. Nature *451*, 596-599.
13. Van Der Spoel, D., Lindahl, E., Hess, B., Groenhof, G., Mark, A.E., and Berendsen, H.J. (2005). GROMACS: fast, flexible, and free. J Comput Chem *26*, 1701-1718.
14. Fulmer, E.C., Mukherjee, P., Krummel, A.T., and Zanni, M.T. (2004). A pulse sequence for directly measuring the anharmonicities of coupled vibrations: Two-quantum two-dimensional infrared spectroscopy. J Chem Phys *120*, 8067-8078.
15. Mukherjee, P., Krummel, A.T., Fulmer, E.C., Kass, I., Arkin, I.T., and Zanni, M.T. (2004). Site-specific vibrational dynamics of the CD3zeta membrane peptide using heterodyned two-dimensional infrared photon echo spectroscopy. J Chem Phys *120*, 10215-10224.
16. Khalil, M., Demirdoven, N., and Tokmakoff, A. (2003). Coherent 2D IR spectroscopy: Molecular structure and dynamics in solution. Journal of Physical Chemistry A *107*, 5258-5279.
17. Mukamel, S. (1995). Principles of Nonlinear Optical Spectroscopy (Oxford, New York).

18. Schmidt, J.R., Corcelli, S.A., and Skinner, J.L. (2005). Pronounced non-Condon effects in the ultrafast infrared spectroscopy of water. Journal of Chemical Physics *123*, 04451301-04451313.
19. Berendsen, H.J.C., Postma, J.P.M., van Gunsteren, W.F., and Hermans, J. (1981). Interaction models for water in relation to protein hydration. In Intermolecular forces, B. Pullman, ed. (Dordrecht: D. Reidel Publishing Company), pp. 331-342.
20. Hu, J., Fu, R., Nishimura, K., Zhang, L., Zhou, H.X., Busath, D.D., Vijayvergiya, V., and Cross, T.A. (2006). Histidines, heart of the hydrogen ion channel from influenza A virus: toward an understanding of conductance and proton selectivity. Proc Natl Acad Sci U S A *103*, 6865-6870.
21. Lindahl, E., Hess, B., and van der Spoel, D. (2001). GROMACS 3.0: a package for molecular simulation and trajectory analysis. Journal of Molecular Modeling *7*, 306-317.
22. Hermans, J., Berendsen, H.J.C., Vangunsteren, W.F., and Postma, J.P.M. (1984). A Consistent Empirical Potential for Water-Protein Interactions. Biopolymers *23*, 1513-1518.
23. Berger, O., Edholm, O., and Jahnig, F. (1997). Molecular dynamics simulations of a fluid bilayer of dipalmitoylphosphatidylcholine at full hydration, constant pressure, and constant temperature. Biophysical Journal *72*, 2002-2013.
24. Hess, B., Bekker, H., Berendsen, H.J.C., and Fraaije, J.G.E.M. (1997). LINCS: A linear constraint solver for molecular simulations. Journal of Computational Chemistry *18*, 1463-1472.
25. Parrinello, M., and Rahman, A. (1981). Polymorphic Transitions in Single-Crystals - a New Molecular-Dynamics Method. Journal of Applied Physics *52*, 7182-7190.
26. Nose, S., and Klein, M.L. (1983). Constant Pressure Molecular-Dynamics for Molecular-Systems. Molecular Physics *50*, 1055-1076.
27. Darden, T., York, D., and Pedersen, L. (1993). Particle Mesh Ewald - an N.Log(N) Method for Ewald Sums in Large Systems. Journal of Chemical Physics *98*, 10089-10092.
28. Lin, Y., Shorb, J.M., Mukherjee, P., Zanni, M.T., and Skinner, J.L. (2008). Biophysical Journal.
29. Jansen, T.L., Dijkstra, A.G., Watson, T.M., Hirst, J.D., and Knoester, J. (2006). Modeling the amide I bands of small peptides. Journal of Chemical Physics *125*, 04431201-04431209.

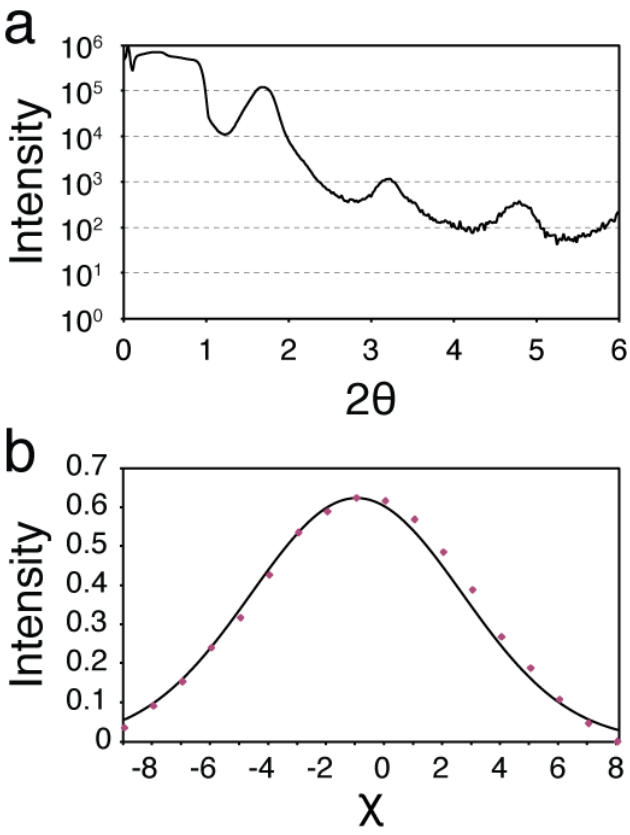

Figure S1. X-Ray Reflectivity and χ Scan of the Peptide
(a) X-ray specular scan of the M2 transmembrane peptide in lipid bilayers.
(b) The χ scan on the first Bragg peak where χ is an angle that is perpendicular to the X-ray beam. The scan measured at this peak is fit to a Gaussian mosaicity function with $\sigma = 2.1°$, and is a measure for the probability distribution of local membrane normal vectors.

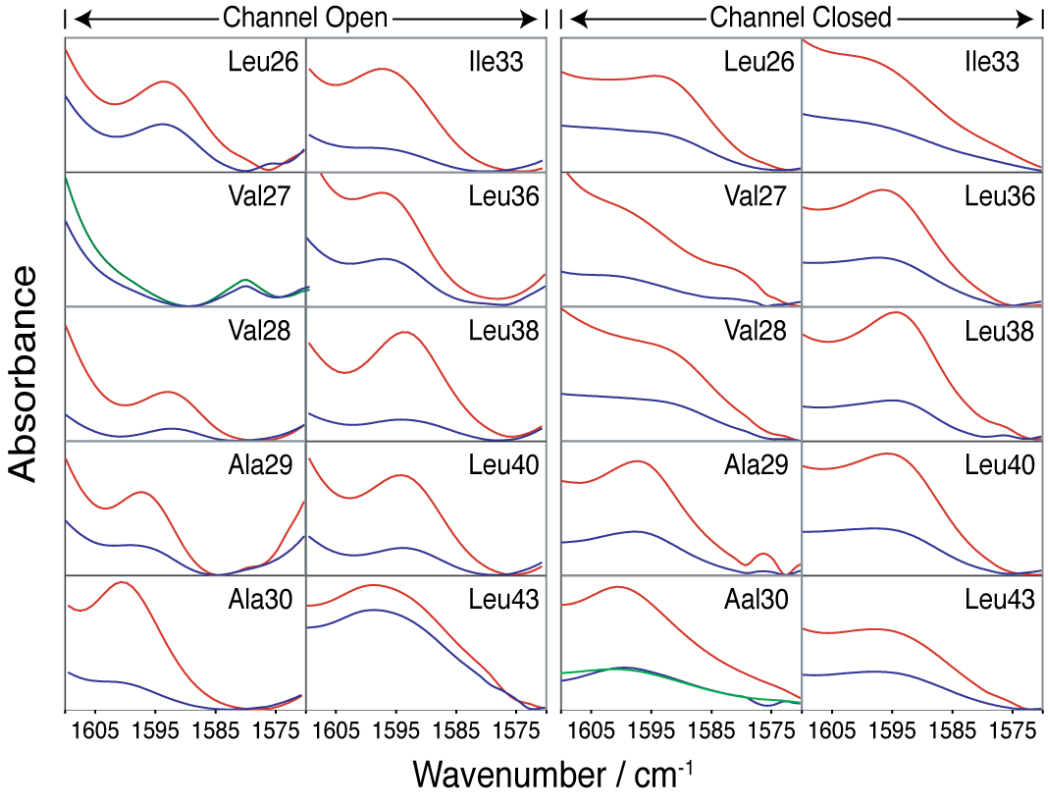

Figure S2. Representative ATR-FTIR Spectra of the M2 Peptide in Lipid Bilayers Focusing on the Isotope-Edited Band of the Amide I Mode
The spectra were collected in parallel or perpendicular polarized light, red and blue curves, respectively. Spectra in green were collected with the polarization plane at an angle of 45° to the membrane plane.

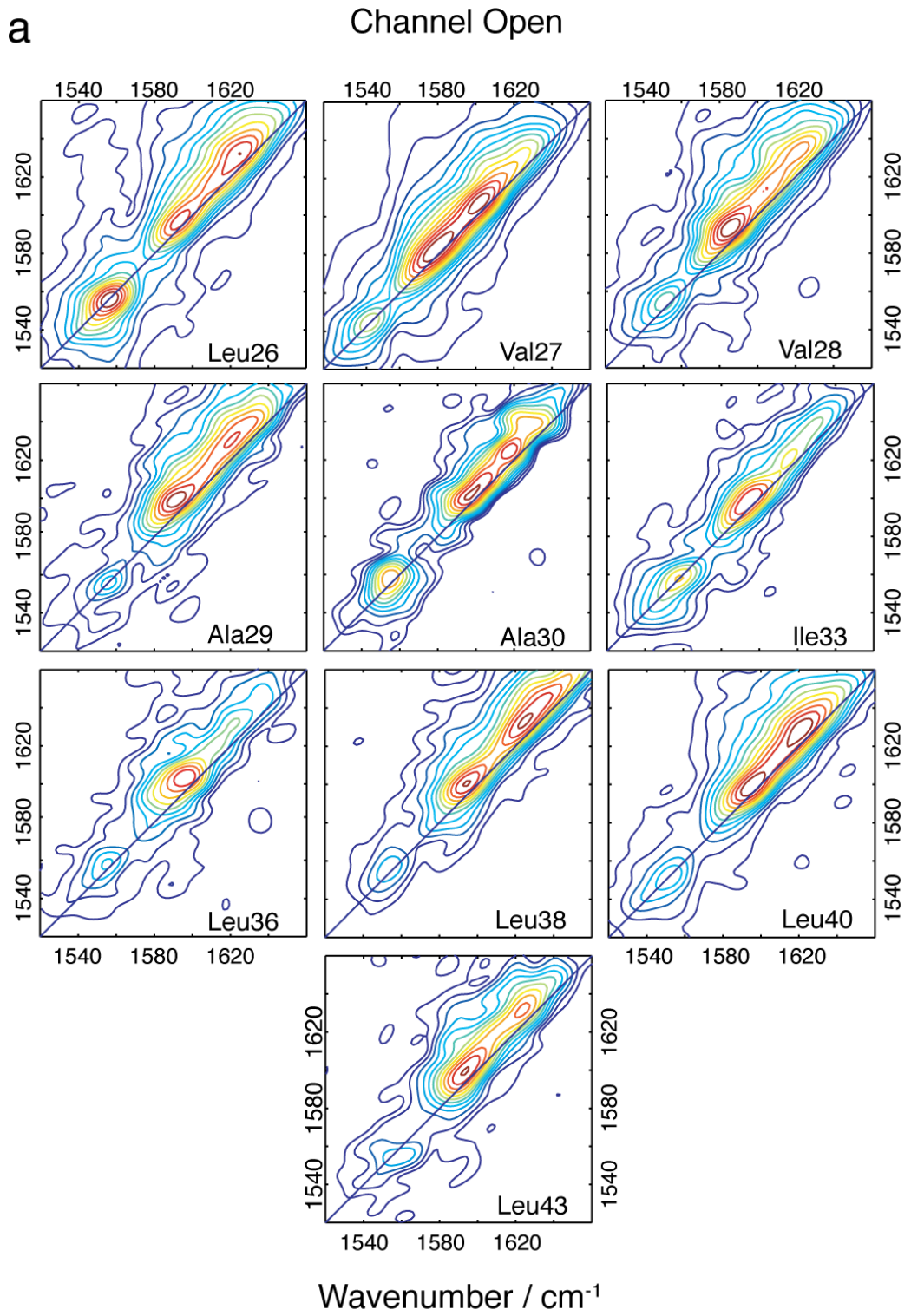
a
Channel Open
1540
1580
1620
Leu26
Val27
Val28
Ala29
Ala30
Ile33
Leu36
Leu38
Leu40
Leu43
Wavenumber / cm-1

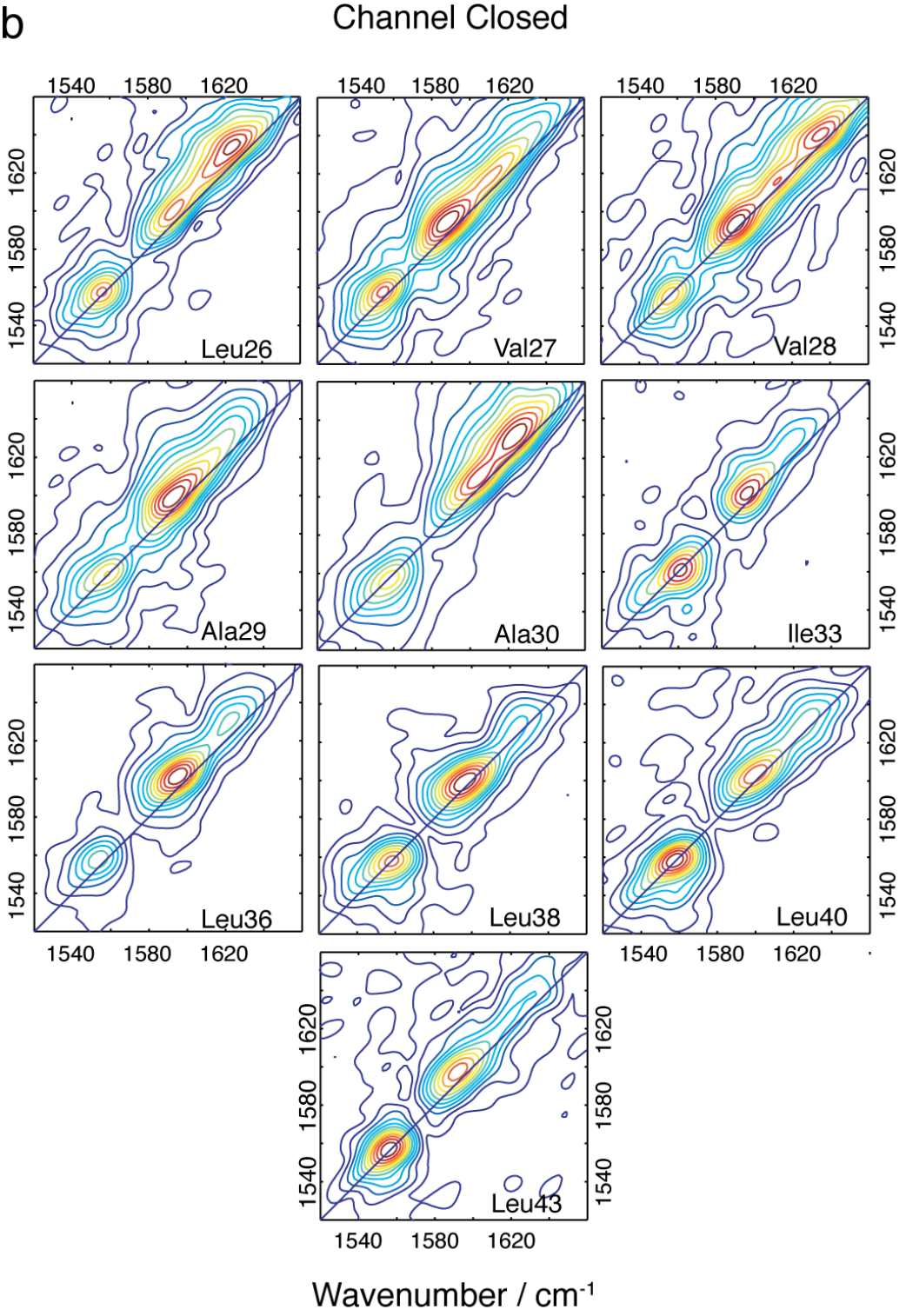

Figure S3. Representative 2D IR Spectra Collected at (a) Low pH and (b) Neutral Conditions for All 10 Residues
60 spectra were collected in total.

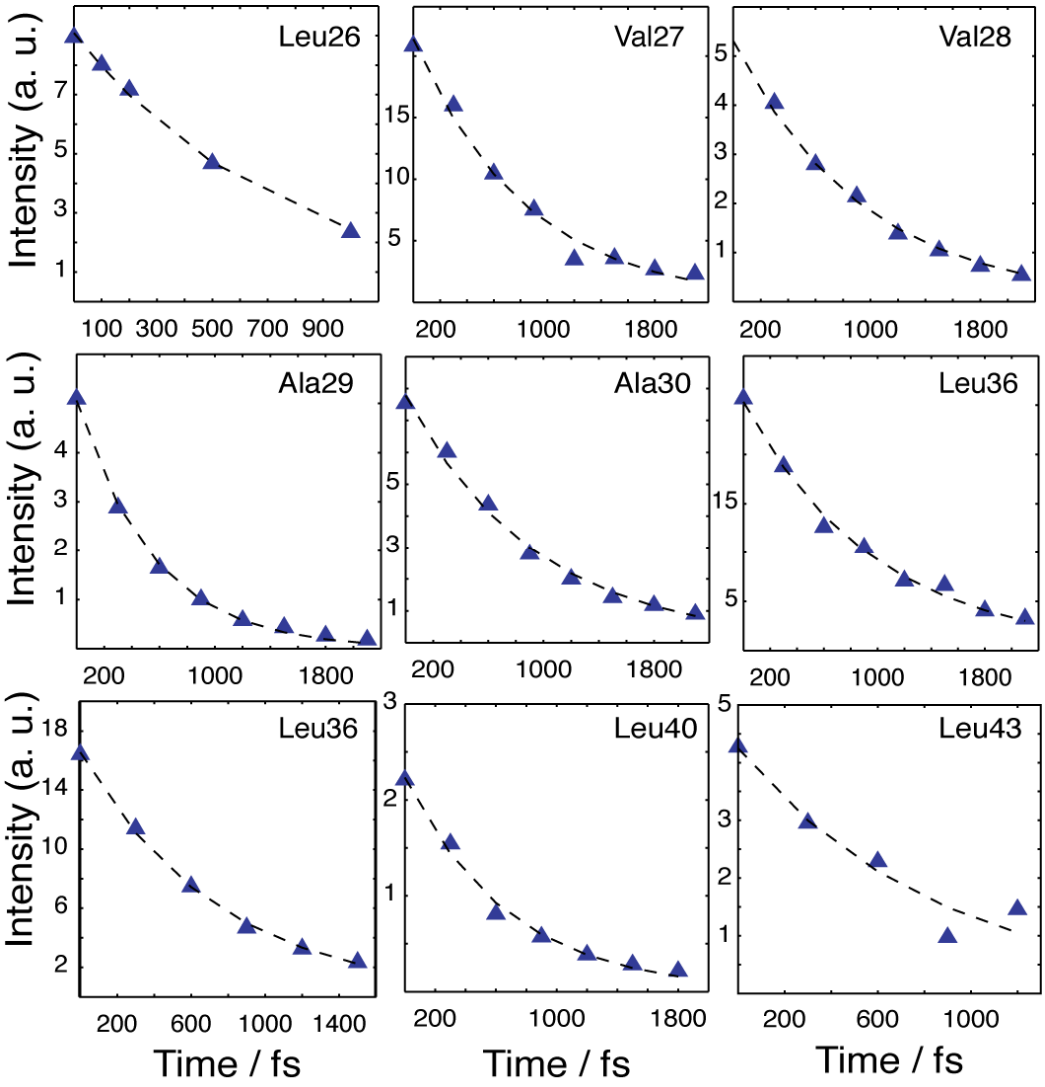

Figure S4. Population Relaxation Measurements at Neutral Conditions
The intensities are generated from a series of 2D IR spectra collected as a function of t_2. The data are fit to single exponentials and the fits are reported in Table S1.

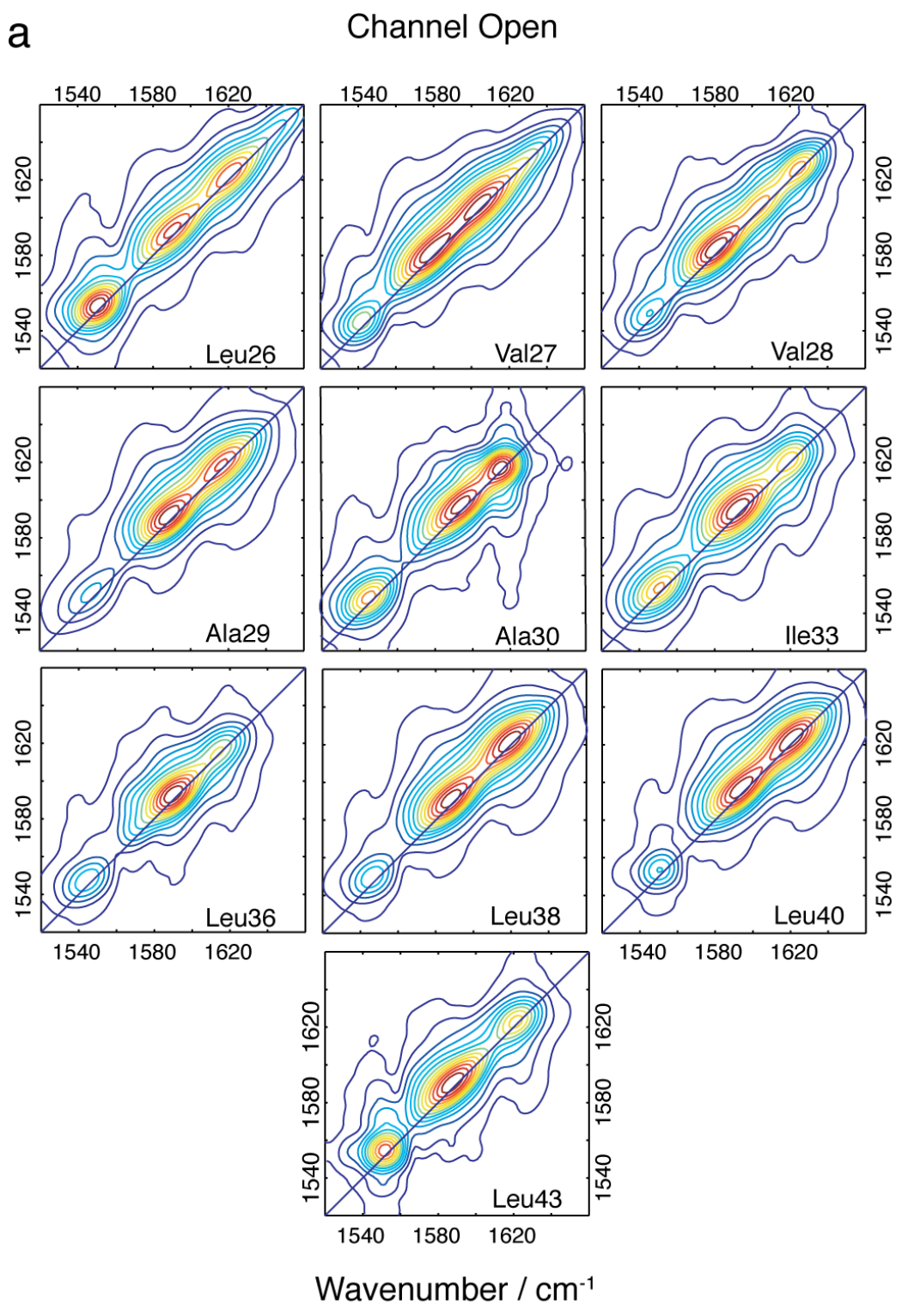
a
Channel Open
1540
1580
1620
Leu26
Val27
Val28
Ala29
Ala30
Ile33
Leu36
Leu38
Leu40
Leu43
Wavenumber / cm-1

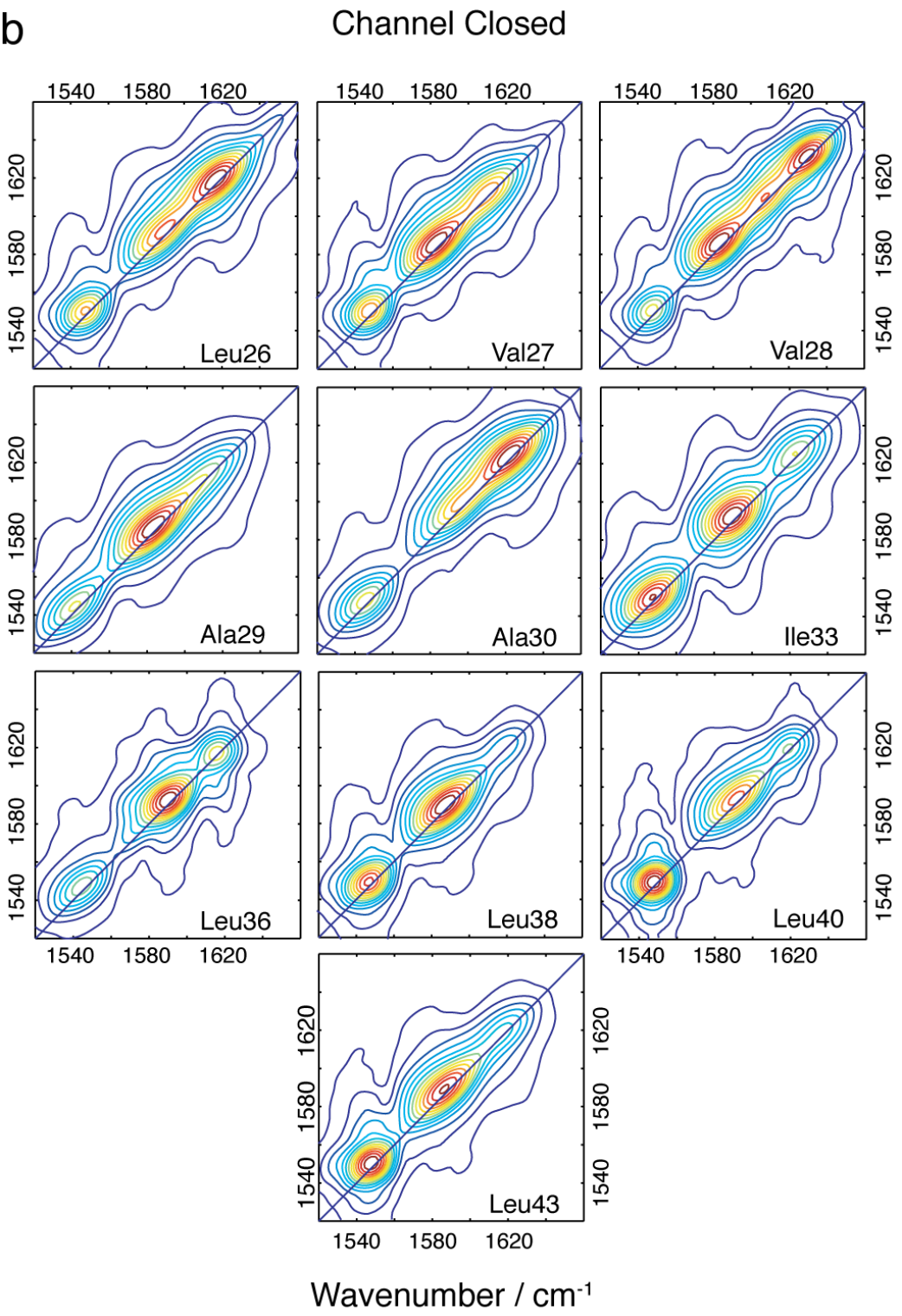

Figure S5. Fits to the 2D IR Spectra Presented in Figure S2, from which the Vibrational Dynamics Parameters Are Extracted and Reported in Table S2
All 60 experimental 2D IR data sets were fit.

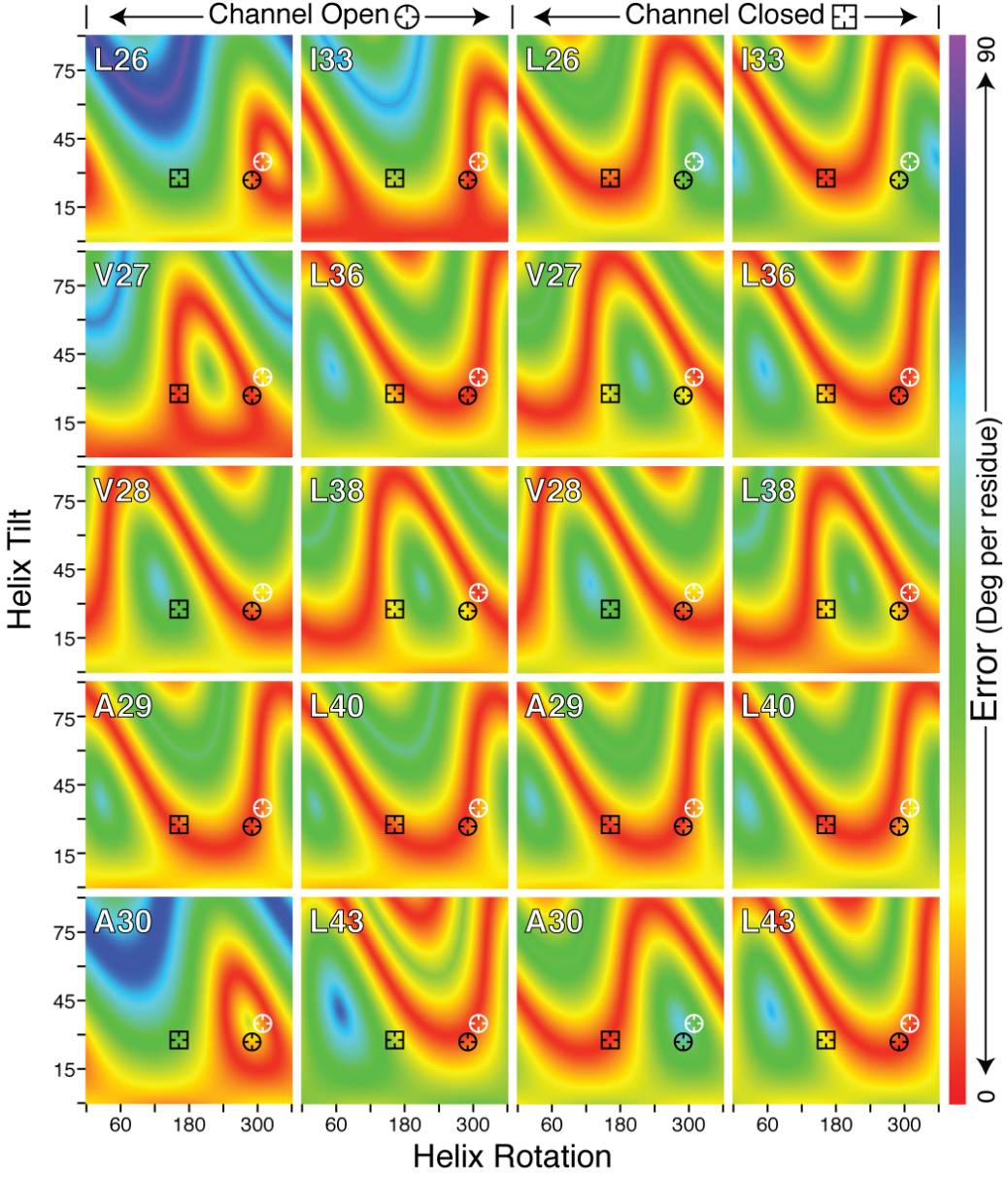

Figure S6. Rigid-Body Refinement of the M2 Protomer According to Individual FTIR Derived Angles

Each point in the graph represents a particular combination of tilt and rotation angles for an ideal helix. The colour scale represents the difference between the angle of the particular residue that the structure has, relative to the angle derived from the FTIR study. The black circle and square represent the helix tilt and rotation combinations that resulted in the smallest deviation form the experimental results, for the closed and open channel data, respectively. The white circle represents the tilt and rotation of the helices of the X-ray structure [12]. Thus it can be seen that there is no individual residue that is solely responsible for the change in structure between the two pH conditions.

Table S1. Experimental Quantities Measured from 2D IR Spectra

Residue Name	Protein in Buffer solution (pH ~5)		Protein in D_2O solution (pH ~ 7)			
	Diagonal Widths (cm^{-1})	Anti-diagonal widths (cm^{-1})	FTIR Absorption Frequencies (cm^{-1})	Diagonal widths (cm^{-1})	Anti-diagonal widths (cm^{-1})	Population relaxation constants at pH 7 (ps)
Leu-26	33.0±0.5	19.0±0.5	1582.5±2	30.5±0.5	14.0±0.5	0.76±0.05
Val-27	30.5±0.5	16.5±0.5	1596.5±2	26.5±0.7	15.0±0.5	0.83±0.05

Val-28	27.5±0.5	15.0±0.5	1601.0±2	25.5±0.5	14.0±0.5	0.94±0.05
Ala-29	26.0±0.5	15.0±0.5	1597.5±2	29.5±0.1	15.0±0.5	0.55±0.05
Ala-30	30.0±0.6	15.0±0.5	1604.5±2	27.0±0.5	15.0±0.5	0.94±0.5
Ile-33	29.0±0.5	15.0±0.5	1601.0±2	24.0±2.0	14.5±0.5	NA
Leu-36	24.5±0.5	15.0±0.5	1598.0±2	22.7±1.0	13.0±0.5	0.99±0.05
Leu-38	29.0±0.7	16.0±0.5	1597.5±2	28.0±2.0	14.5±0.5	0.75±0.05
Leu-40	29.0±0.6	14.0±0.5	1599.0±2	30.0±2.0	14.0±0.5	0.69±0.05
Leu-43	31.0±1.0	18.0±0.5	1586.0±2	29.5±1.0	15.5±0.5	0.86±0.05

Frequencies are measured from FTIR spectra. Lifetimes are generated by single exponential fits (see Figure S4).

Table S2. Homogeneous and Inhomogeneous Broadening Parameters Extracted from Fits to the 2D IR Spectra

Residue Name	Protein in Buffer solution (pH ~5)		Protein in D_2O solution (pH ~ 7)	
	T_2^* (ps)	Δ_0 (ps^{-1})	T_2^* (ps)	Δ_0 (ps^{-1})
Leu-26	2.6±2	1.6±0.05	2.6±2	1.55±0.05
Val-27	15.4±5	1.57±0.05	15.4±5	1.30±0.03
Val-28	15.4±5	1.35±0.05	15.4±5	1.10±0.02
Ala-29	15.4±5	1.10±0.02	15.4±5	1.40±0.03
Ala-30	2.6±2	1.56±0.05	2.6±5	1.40±0.05
Ile-33	0.3±0.1	1.40±0.05	0.3±0.1	1.00±0.02
Leu-36	15.4±5	1.10±0.02	15.4±5	0.90±0.02
Leu-38	15.4±5	1.35±0.02	15.4±5	1.35±0.03
Leu-40	15.4±5	1.35±0.02	15.4±5	1.40±0.05
Leu-43	15.4±5	1.50±0.05	15.4±5	1.45±0.05

Table S3. Diagonal Linewidths and Errors Predicted from Simulations

Residue	Calculated diagonal widths (cm^{-1})
22	39.6 ± 3.5
23	33.2 ± 4.1
25	21.9 ± 1.4
26	29.1 ± 5.2
27	37.5 ± 2.5
28	16.9 ± 1.3
29	19.6 ± 0.8
30	36.7 ± 0.8
31	21.3 ± 4.1
32	18.2 ± 0.3
33	29.9 ± 2.8
34	19.6 ± 2.1
35	21.0 ± 1.6
36	19.1 ± 1.0
37	21.3 ± 0.6
38	16.8 ± 0.4
39	17.0 ± 0.6
40	17.0 ± 1.6
41	19.1 ± 1.8
42	17.5 ± 1.1
43	22.9 ± 1.4
44	29.4 ± 2.4
45	29.8 ± 2.1

Residue 24 is not included because its amide I bond lacks a N-H group since it is formed with Pro-25.